Since January 2020 Elsevier has created a COVID-19 resource centre with free information in English and Mandarin on the novel coronavirus COVID-19. The COVID-19 resource centre is hosted on Elsevier Connect, the company's public news and information website.

Synthesis, molecular docking, and *in silico* ADME/Tox profiling studies of new 1-aryl-5-(3-azidopropyl)indol-4-ones: Potential inhibitors of SARS CoV-2 main protease

Francisco Xavier Domínguez-Villa [a], Noemi Angeles Durán-Iturbide [a], José Gustavo Ávila-Zárraga [a,*]

[a] *Facultad de Química, Universidad Nacional Autónoma de México, Circuito Exterior, Ciudad Universitaria, 04510 Coyoacán, DF, Mexico*

A R T I C L E   I N F O

A B S T R A C T

The virus SARS CoV-2, which causes the respiratory infection COVID-19, continues its spread across the world and to date has caused more than a million deaths. Although COVID-19 vaccine development appears to be progressing rapidly, scientists continue the search for different therapeutic options to treat this new illness. In this work, we synthesized five new 1-aryl-5-(3-azidopropyl)indol-4-ones and showed them to be potential inhibitors of the SARS CoV-2 main protease (3CLpro). The compounds were obtained in good overall yields and molecular docking indicated favorable binding with 3CLpro. *In silico* ADME/Tox profile of the new compounds were calculated using the *SwissADME* and *pkCSM-pharmacokinetics* web tools, and indicated adequate values of absorption, distribution and excretion, features related to bioavailability. Moreover, low values of toxicity were indicated for these compounds. And drug-likeness levels of the compounds were also predicted according to the Lipinski and Veber rules.

1. Introduction

In December 2019, a contagion of atypical and severe pneumonia was first reported in Wuhan, Hubei Province, China and has since widely spread worldwide [1]. This new disease was subsequently attributed to a new class of coronavirus, specifically severe acute respiratory syndrome coronavirus 2 (SARS CoV-2), which probably emerged as a zoonotic disease from bats or pangolins, and was named coronavirus disease 2019 (COVID-19) [2]. By the end of January 2020 the outbreak was declared a Public Health Emergency of International Concern by the World Health Organization [3].

COVID-19 causes symptoms such as dry cough, headache, fever, difficult breathing (dyspnea), and pneumonia, which can trigger respiratory failure and as a result death [4]. To date, no highly effective therapy for treating coronavirus infections has been made available, so many research groups worldwide are working to develop therapeutic options to fight this pathogen. Some structural elements of SARS CoV-2 have been identified *in silico* as possible therapeutic targets [5–7]. The most promising targets so far identified have been the spike protein, RNA-dependent RNA polymerase (RdRp), and the papain-like protease

3CLpro, also known as main protease (Mpro) [8,9]. Mpro is interesting because it is fundamental for the life cycle of SARS CoV-2 [2] and the absence of homologous proteins in humans make it an attractive target for the development of new antiviral drugs.

The catalytic site of 3CLpro is a dimeric unit containing a Cys-Hys dyad [10]. The thiol group in Cys acts as a nucleophile in the proteolytic process. So the inhibition of 3CLpro can be achieved using peptidic inhibitors containing electrophilic groups such as epoxides, ketones, aldehydes and Michael acceptors [11].

In this context, organic azides (R-N$_3$) are groups with an electrophilic behavior. As illustrated in Scheme 1, the nitrogen directly attached to the organic group (labeled **a**) can work as a nucleophile and the distal nitrogen (**c**) shows electrophilic reactivity [12]. Zidovudine is an example of an antiviral containing the azide group, and the presence of the –N$_3$ functional group (specifically the presence of nitrogen **c**) is determinant for the interaction of the antiviral with its reverse transcriptase pharmacological target [13,14].

Also, indolones constitute an important family of fused heterocycles with potential for use against SARS CoV-2. They are found in many natural products [15] and drugs [16], and show diverse biological

Scheme 1. Structure of the alkyl azide.
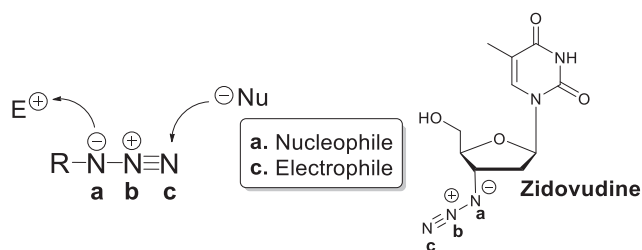
activities such as anti-inflammatory [17], antihypertensive [18] and antiproliferative [19] activities. Indolones were shown in 2005 to potently inhibit 3CLpro of SARS CoV [20].

In the work described here, we synthesized of a new set of compounds with potential as inhibitors of the SARS CoV-2 3CLpro. These compounds were designed to each link as key fragments an azide group and the indolone skeleton and hence provide a strategy for presenting a positive synergic effect in their interactions with 3CLpro. We also performed molecular dockings of azidopropylindolones with protease 3CLpro of SARS CoV-2 as well as *in silico* ADME/Tox profilings to propose a possible therapeutic option to treat COVID-19.

2. Syntheses

The syntheses of the current work were carried out as shown in Scheme 2.

The synthesis of compound **1** was achieved by alkylating dimedone using chloroacetone with potassium carbonate dissolved in chloroform. Then Paal-Knorr reactions each using a different *p*-substituted aniline were performed to yield a set of 1-aryl-4-indolones [21].

Compounds **2** were treated with LDA in anhydrous THF to generate the corresponding enolates, which were afterwards subjected to alkylation reactions with 1-chloro-3-iodopropane to generate compounds **3** [22].

We then set out to replace the chlorine atom of each compound **3** with an azide group. First a substitution reaction starting with a catalyst-free assay was attempted (Table 1, **Entry 1**). In this case, the reaction took more than 72 h. Due to these results, a double substitution using potassium iodide was implemented. The presence of the iodide in the reaction media resulted in a decrease in the reaction time, to as low as 48 h when 0.2 equivalents of KI were used (Table 1, **Entry 5**). When using a compound more soluble in DMF such as TBAI, the reaction time decreased to 16 h (Table 1, **Entry 6**).

Once the reaction conditions were defined, the syntheses producing the new family of azidopropylindolones were achieved with excellent
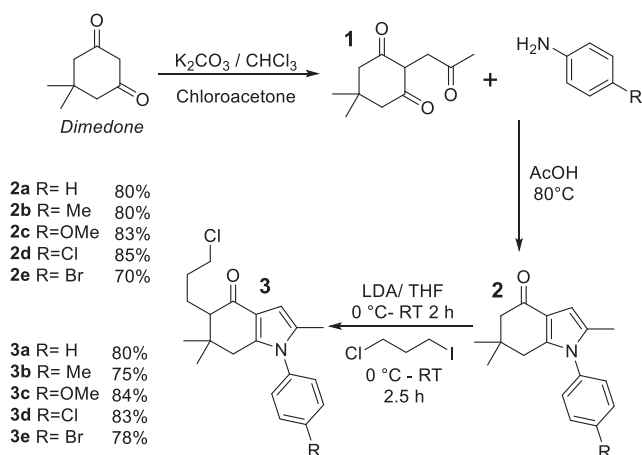
Scheme 2. Synthetic route for chloropropylindolones.

Table 1
Evaluation of the catalyst amount for the chlorine substitution.

Entry	Iodide source	Eq I$^-$	t(h)	4a (%)
1	KI	0	<72	92
2	KI	0,05	72	97
3	KI	0,1	72	96
4	KI	0,15	56	99
5	KI	0,2	48	99
6	TBAI	0.2	16	95

yields. The overall yields were about 50% (Table 2), which suggested that the designed methodologies were efficient.

3. Molecular dockings of azidopropylindolones with 3CLpro

3.1. Receptor preparation

The structure of 3CLpro of SARS CoV-2 was downloaded from the Protein Data Bank (PDB ID: 6Lu7) [8] and visualized using Chimera-1.14. The nonproteinic residues were removed, and then the structure was subjected to a minimization using AMBER ff14SB as the force field, with 500 cycles of steepest descent and 100 of the conjugate gradient method. Then the file was saved as Mpro.pdb.

3.2. Ligand preparation

Ligand geometry was refined using the PBE1PBE / 6–31+(d,p) density functional model, with an empirical dispersion of GD3 in Gaussian 09.

3.3. Molecular dockings

The molecular dockings were carried by using the AutoDockTools-1.5.6 suite and PyMol 1.8 as a visualizer. The rotatable bonds of the ligands were considered, but the macromolecule (3CLpro) was considered to be rigid. A 60x60x60-point grid with a gap of 0.375 Å was established and the coordinates of the co-crystallized ligand binding site were used to center the preset grid; the results are presented in Table 3.

All compounds showed negative values of binding energy. This result suggested the favorability of their interactions with the 3CLpro active site. In fact, their binding energies were calculated to all be lower than −6.6 kcal/mol. The most outstanding binding energy values were calculated for derivatives **4c** and **4e.**

The dockings of compounds **4c, 4d,** and **4e** showed interactions

Table 2
Yields and overall yields in the synthesis of azidopropylindolones.

	R	Yield of the last step(%)	Overall yield (%)
4a	H	95	52.3
4b	Me	92	47.5
4c	OMe	94	56.4
4d	Cl	90	54.6
4e	Br	88	41.3

Table 3
Interaction of the SARS CoV-2 main protease (3CLpro) with the azidopropylindolones.

4a R= H
4b R= Me
4c R=OMe
4d R=Cl
4e R= Br

	ΔG (Kcal/mol)	Interactions
4a	−6.8	N₃ - Leu27
4b	−6.76	N₃ - Leu 4
4c	−7.73	N₃ - Thr25 Cys 44, Met-49; *p*-Ome - Hys163
4d	−6.67	N₃ - Thr 26
4e	−7.26	N₃ - Thr25; *p*-Br Hys163

between the azide group and the key residues Thr25, Thr26 and Cys44. These interactions have already been predicted from docking studies of other potential inhibitors of 3CLpro [23]. Of the five compounds **4** tested, the binding of the azidopropylindolone **4c** for 3CLpro was calculated to be the strongest. In the docked structure, the distal nitrogen atom (c) of its azide group showed specific interactions with the hydroxyl group of Thr25, carbonyl and thiol groups of Cys44, and sulfur atom in Met49. Furthermore, its pyrrole nitrogen formed an interaction with the carbonyl carbon of Asn142, and the methoxy group at the *para* position of its aromatic ring formed a hydrogen bond with residue His163 (Fig. 1).

4. ADME/Tox profile

ADME/Tox is used to describe the absorption, distribution, metabolism, excretion and toxicity of drugs. The *in silico* ADME/Tox profile is a useful tool to predict the pharmacological and toxicological properties of drug candidates, especially in pre-clinical stages. To improve ADME/Tox predictions, *in silico* models have been deployed. Use of these models has specifically been contributing to drug optimization and avoiding late-stage failures, also are important since such failures cause considerable unproductive investment of time and money [24].

4.1. ADME/Tox web tools

The freely accessible *SwissADME* web tool (http://www.swissadme. ch/) assembles the most relevant computational methods to provide a global appraisal of the pharmacokinetics profile of small molecules. The methods were selected by the web tool designers for robustness, but also for ease of interpretation to enable efficient translation to medicinal

chemistry. Some of these methods were modified by the web tool designers using open-source algorithms, and others were unmodified versions of the methods from the original authors [25].

The freely accessible *pkCSM-pharmacokinetics* web tool (http://structure.bioc.cam.ac.uk/pkcsm) is a novel method for predicting and optimizing small-molecule ADME/Tox properties and relies on graph-based signatures and experimental data [26].

These web tools provide in the literature methods design description, methods validation information, and for most methods provide information of the datasets used.

ADME/Tox profile calculation

The molecular structures of the synthetized azidopropylindolones (**4a**, **4b**, **4c**, **4d**, **4e**) were introduced in simplified molecular-input line-entry specification (SMILES) nomenclature into the ADME/Tox web tools *SwissADME and pkCSM-pharmacokinetics.* We selected the most important ADME/Tox properties provided from the web tools to represent the ADME/Tox profile.

4.2. ADME/Tox profile

Absorption was predicted from water solubility, lipophilicity and percentage of intestinal human absorption (HIA) properties. Water solubility was predicted using the Silicos IT LogSw descriptor of *SwissADME*. LogSw values for our compounds were predicted to range from −6.28 to −7.34. In the *SwissADME* LogSw scale, compounds with values less than (more negative than) −6 are considered to be poorly soluble. Lipophilicity was assessed using the logarithm of the *n*-octanol/water partition coefficient, which was predicted using the Consensus LogP$_{o/w}$ descriptor of *SwissADME*. LogP$_{o/w}$ is closely related to transport processes, including membrane permeability, and distribution to different tissues and organs [27]. A general guide for good oral bioavailability (good permeability and solubility) is to have a moderate logP ($0 < \log P < 3$) [28]. For our compounds, the predicted values of logP$_{o/w}$ ranged from 3.79 to 4.74.

The logSw and logP$_{o/w}$ predictions indicated a correlation between solubility and lipophilicity. The percentages of the newly synthesized azidopropylindolones that would be absorbed through the human intestine (% HIA) were predicted using *pkCSM-pharmacokinetics* to range from 91.11 to 94.81% (see bar plot in Fig. 2), and hence to be adequate.

Distribution was predicted using the glycoprotein P (P-gp) substrate, blood–brain barrier (BBB) permeability and fraction unbound descriptors. Descriptors were predicted using *pkCSM-pharmacokinetics*. P-gp is an ATP-dependent drug-extracting pump, and it is found in various human tissues. All of the new synthesized molecules were predicted to be substrates of P-gp.

The BBB is a complex structure that separates the central nervous system (CNS) from the peripheral tissue. In order to maintain homeostasis in the CNS, the BBB controls the transfer of material, nutrients and cells from the blood to the brain and from the brain to the blood. It also
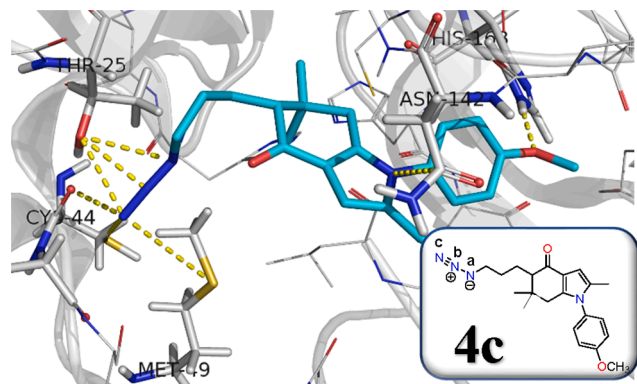

Fig. 1. Molecular docking of SARS CoV-2 main protease (3CLpro) and **4c** and interactions with key residues.
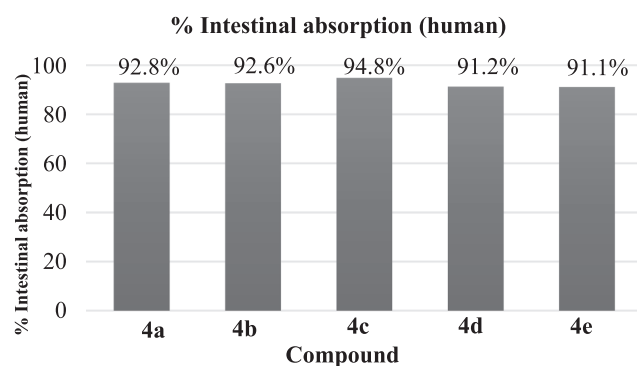

Fig. 2. Percentages of the synthesized compounds predicted to be absorbed through the human intestine (% HIA) using *pkCSM-pharmacokinetics*.

participates in the clearance of cellular metabolites and toxins from the brain to the blood [29]. BBB permeability values of our compounds were predicted to range from −0.38 to −0.67.

Most drugs in plasma exist in equilibrium between an unbound state and a state in which they are bound to serum proteins. The fraction of drug molecules in the plasma that are not bound to protein (denoted as "fraction unbound") influences renal glomerular filtration and hepatic metabolism, and consequently affects the volume of distribution, total clearance, and efficacy of drugs [30]. The greater the degree to which the drug binds proteins in the blood, the less efficiently it can diffuse/ pass through cell membranes [26]. In the current work, fraction unbound values were predicted for the five azidopropylindolones in human plasma to have low values, specifically between 0.035 and 0.081 (Fig. 3).

Metabolism was estimated using *SwissADME* according to inhibition of the main cytochromes (CYP) of the P450 superfamily, namely CYP1A2, CYP2C19, CYP2C9, CYP2D6 and CYP3A4. CYP enzyme inhibition, a principal mechanism for metabolism-based drug–drug interactions, usually involves competition with another drug for the same enzyme binding site. Enzyme inhibition impairs the biotransformation or clearance of all clinically used drugs including several anticancer agents, resulting in higher plasma levels of drugs that influence the therapeutic outcome. If the drug is a prodrug, then the effect is decreased. Thus, inhibition of CYPs may lead to toxicity or lack of efficacy of a drug [31]. CYP2C19 metabolizes several drugs and is involved in the detoxification of potential carcinogens or bioactivation of some environmental procarcinogens [32]. CYP2C9 is the major enzyme that metabolizes drugs with a narrow therapeutic index [33]. CYP2D6 is highly polymorphic and its metabolism is variable; people with reduced or no activity of this enzyme would be at risk of reduced efficacy of drugs or present adverse effects [34]. Molecules **4a** and **4c** were predicted to likely inhibit CYP1A2, and all five synthesized azidopropylindolones probably inhibit CYP2C19, CYP2C9 and CYP3A4; in contrast, the compounds were predicted to not inhibit CYP2D6.

Excretion occurs primarily as a combination of hepatic and renal clearance, is related to bioavailability, and is important for determining dosing rates to achieve steady-state concentrations [26]. Excretion values were predicted, using the total clearance (CLtot) descriptor of *pkCSM-pharmacokinetics*, to range from 0.02 to 0.138 ml/min/kg.

The toxicity levels of the synthesized compounds were predicted by using *pkCSM-pharmacokinetics* to predict hepatotoxicity and oral rat acute toxicity LD50 values [26]. Predicted LD50 values ranged from 2.504 to 2.649 mol/kg. The liver plays a critical role in energy exchanges and the biotransformation of xenobiotics and drugs. Liver suffering from damage always disrupts normal metabolism and could even lead to liver failure [35]. The hepatotoxicity descriptor predicted that molecules **4a**, **4b**, **4c** could present hepatotoxicity.

Drug-likeness descriptors selected using the Lipinski and Veber rules were calculated with *SwissADME*. The rule of five by Lipinski argues that good absorption or permeation is more likely when the molecular weight (MW) < 500 Da, number of hydrogen bond donors (HBDs) < 5 as shown in molecular docking studies, LogP < 5, and number of hydrogen bond acceptors (HBAs) < 10. Veber et al. identified two other relevant descriptors: number of rotatable bonds (NBR) < 10 and polar surface area (PSA) < 140 Å^2 [29]. Analyses of the new synthesized molecules indicated no violations of these rules, suggesting that they would display well-behaved absorption or permeation.

4.3. Target prediction

Nowadays, efficient support to estimate most probable targets of small molecules can be provided by established bio-/chemo-informatics approaches. Ligand-based target prediction has shown high-quality performance and the ability to quickly predict correct protein targets of compounds in drug discovery contexts [36]. Predictions made using the *SwissTarget* web tool aims to predict the most probable protein targets of small molecules.

The current analysis was restricted to the top 15 *Homo sapiens* targets. Molecule **4a** was estimated to have a 33.3% probability of binding family A G protein-coupled receptors. Molecule **4b** was predicted to have a 26.7% probability of binding two receptors: voltage-gated ion channels and family A G protein-coupled receptors. Molecule **4c** was predicted to have a 13.3% probability of binding six different receptors (Supplementary material). Molecule **4d** was predicted to have a 20% probability of binding voltage-gated ion channels and 13.3% probability of binding proteases (Fig. 4). Finally, molecule **4e** was predicted to have a 20% probability of binding voltage-gated ion channels and 13.3% probability of binding proteases, as predicted in the molecular docking studies.

5. Conclusions

In summary, five new compounds were obtained, each in a four-step synthetic pathway, with overall yields of up to 50% in most of the cases. The final reaction of this short route yielded the 1-aryl-5-(3-azidopropyl) indol-4-ones in excellent yields (88–95%).

The five synthesized compounds showed favorable calculated values of interaction energy in the molecular docking with the SARS CoV-2 main protease 3CLpro. The presence of the azide group was indicated to be essential for the interaction with the key residues of the active site of the protease known so far. Likewise, the formation of hydrogen bonding between the methoxy group of compound **4c** and the 3CLpro protease was indicated to have accounted for the relatively strong calculated binding of this compound for the protease.

The ADME/Tox analysis predicted good lipophilicity values, low fraction unbound values, and adequate distributions for most of the
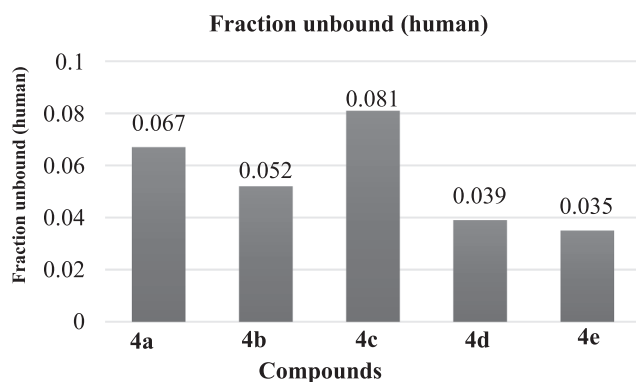

Fig. 3. Fraction unbound values of the tested compounds in human plasma as predicted using *pkCSM-pharmacokinetics*.
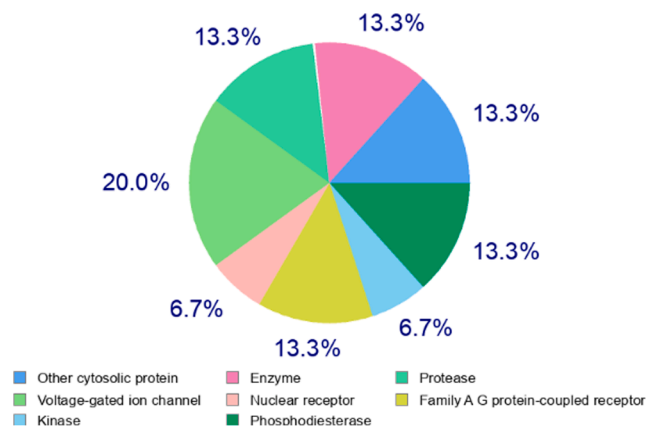

Fig. 4. Top 15 targets of 4d as predicted using SwissTarget.

compounds, and therefore fine bioavailability levels are expected. As for metabolism, the compounds could not inhibit CYP2D6, which is a determinant in biotransformation processes. Finally, total clearance values of 0.02 to 0.138 ml/min/kg were predicted for the compounds, with total clearance also related to bioavailability. The compounds were predicted to display low toxicity levels. And each of the compounds showed drug-likeness according to the Lipinski and Veber rules.

Declaration of Competing Interest

The authors declare that they have no known competing financial interests or personal relationships that could have appeared to influence the work reported in this paper.

Acknowledgements

We are grateful for the PAIP project 5000:9060. UNAM USAII technicians are also thanked.

Appendix A. Supplementary material

Supplementary data to this article can be found online at https://doi.org/10.1016/j.bioorg.2020.104497.

References

[1] T. Phan, Infect. Genet. Evol. 79 (2020), 104211.
[2] A. Wu, Y. Peng, B. Huang, X. Ding, X. Wang, P. Niu, J. Meng, Z. Zhu, Z. Zhang, J. Wang, J. Sheng, L. Quan, Z. Xia, W. Tan, G. Cheng, T. Jiang, Cell Host Microbe 27 (2020) 325.
[3] J. Guarner, Am. J. Clin. Pathol. 153 (2020) 420.
[4] H.A. Rothan, S.N. Byrareddy, J. Autoimmun. 109 (2020), 102433.
[5] A. Wu, Y. Liu, Y. Yang, P. Zhang, W. Zhong, Y. Wang, Q. Wang, Y. Xu, M. Li, X. Li, M. Zheng, L. Chen, H. Li, Acta Pharm. Sin. B 10 (2020) 766.
[6] C.J. Cortés-García, L. Chacón-García, J.E. Mejía-Benavides, E. Díaz-Cervantes, PeerJ Physical Chemistry 2 (2020), e10.
[7] R. Ling, Y. Dai, B. Huang, W. Huang, J. Yu, X. Lu, Y. Jiang, Peptides 130 (2020), 170328.
[8] Z. Jin, X. Du, Y. Xu, Y. Deng, M. Liu, Y. Zhao, B. Zhang, X. Li, L. Zhang, C. Peng, Y. Duan, J. Yu, L. Wang, K. Yang, F. Liu, R. Jiang, X. Yang, T. You, X. Liu, X. Yang, F. Bai, H. Liu, X. Liu, L.W. Guddat, W. Xu, G. Xiao, C. Qin, Z. Shi, H. Jiang, Z. Rao, H. Yang, Nature 582 (2020) 289.
[9] T. Pillaiyar, M. Manickam, V. Namasivayam, Y. Hayashi, S.-H. Jung, J. Med. Chem. 59 (2016) 6595.
[10] J. He, L. Hu, X. Huang, C. Wang, Z. Zhang, Y. Wang, D. Zhang, W. Ye, Int. J. Antimicrob. Agents (2020), 106055.
[11] F. Wang, C. Chen, W. Tan, K. Yang, H. Yang, Sci. Rep. 6 (2016) 22677.
[12] S. Bräse, C. Gil, K. Knepper, V. Zimmermann, Angew. Chem. Int. Ed. Engl. 44 (2005) 5188.
[13] H.D. Langtry, D.M. Campoli-Richards, Drugs 37 (1989) 408.
[14] P.A. Furman, D.W. Barry, Am. J. Med. 85 (1988) 176.
[15] T. Yan, W. Wu, T. Su, J. Chen, Q. Zhu, C. Zhang, X. Wang, B. Bao, Arch. Pharm. Res. 38 (2015) 1530.
[16] H. Ibrahim, A. Furiga, E. Najahi, C. Pigasse Hénocq, J.-P. Nallet, C. Roques, A. Aubouy, M. Sauvain, P. Constant, M. Daffé, F. Nepveu, J. Antibiot. 65 (2012) 499.
[17] F. Breedveld, Scand. J. Rheumatol. Suppl. 100 (1994) 31.
[18] A. Dorszewski, B. Müller-Beckmann, L. Kling, G. Sponer, Br. J. Pharmacol. 101 (1990) 686.
[19] R. Martínez, J.G. Avila, M.T. Ramírez, A. Pérez, A. Martínez, Bioorg. Med. Chem. 14 (2006) 4007.
[20] L.-R. Chen, Y.-C. Wang, Y.W. Lin, S.-Y. Chou, S.-F. Chen, L.T. Liu, Y.-T. Wu, C.-J. Kuo, T.-S.-S. Chen, S.-H. Juang, Bioorg. Med. Chem. Lett. 15 (2005) 3058.
[21] G.R. Proctor, B.G. Mc.Donald, J. Chem. Soc., Perkin Trans. 1 (1446) 1975.
[22] F. Xavier Domínguez-Villa, G. Ávila-Zárraga, C. Armenta-Salinas, Tetrahedron Lett. 61 (2020), 151751.
[23] S. Kumar, P.P. Sharma, U. Shankar, D. Kumar, S.K. Joshi, L. Pena, R. Durvasula, A. Kumar, P. Kempaiah, B. Rathi Poonam, J. Chem. Inf. Model. (2020).
[24] N.A. Durán-Iturbide, B.I. Díaz-Eufracio, J.L. Medina-Franco, ACS Omega 26 (2020) 16076.
[25] A. Daina, O. Michielin, V. Zoete, Sci. Rep. 7 (2017) 42717.
[26] D.E.V. Pires, T.L. Blundell, D.B. Ascher, J. Med. Chem. 58 (2015) 4066.
[27] H. Van de Waterbeemd, in:, Comprehensive Medicinal Chemistry II, Elsevier, 2007, pp. 669–697.
[28] A. Zerroug, S. Belaidi, I. BenBrahim, L. Sinha, S. Chtita, J. King Saud Univ. – Sci. 4 (2018) 595.
[29] M.A. Małkiewicz, A. Szarmach, A. Sabisz, W.J. Cubała, E. Szurowska, P.J. Winklewski, J. Neuroinflammation 16 (2019) 15.
[30] R. Watanabe, T. Esaki, H. Kawashima, Y. Natsume-Kitatani, C. Nagao, R. Ohashi, K. Mizuguchi, Mol. Pharm. 15 (2018) 5302.
[31] P. Manikandan, S. Nagini, Curr. Drug Targets 19 (2018) 38.
[32] Z. Wang, H. Yang, Z. Wu, T. Wang, W. Li, Y. Tang, G. Liu, ChemMedChem 13 (2018) 2189.
[33] A.K. Daly, A.E. Rettie, D.M. Fowler, J.O. Miners, J. Pers. Med. 8 (2017).
[34] A.L. Del Tredici, A. Malhotra, M. Dedek, F. Espin, D. Roach, G.-D. Zhu, J. Voland, T.A. Moreno, Front. Pharmacol. 9 (2018) 305.
[35] A. Daina, O. Michielin, V. Zoete, Nucleic Acids Res. 47 (2019) W357.
[36] S. He, T. Ye, R. Wang, C. Zhang, X. Zhang, G. Sun, X. Sun, Int. J. Mol. Sci. 20 (2019).